

Influence of citric acid on formation of Ni/NiO nanocomposite by sol–gel synthesis

Kamaraj Mahendraprabhu · Perumal Elumalai

Received: 4 July 2014 / Accepted: 17 October 2014 / Published online: 28 October 2014
© Springer Science+Business Media New York 2014

Abstract Nickel/nickel oxide (Ni/NiO) nanocomposite was synthesized by simple sol–gel process by using nickel nitrate as a precursor and citric acid as a gelling agent. The obtained samples were characterized by X-ray diffraction (XRD), scanning electron microscope (SEM), energy dispersive X-ray analysis, Fourier transformed infra-red spectroscopy and vibrating sample magnetometer studies. The influence of citric acid on the formation of Ni/NiO composition was primarily studied by varying the mole ratios of nickel nitrate and citric acid ((N:C) : 1:1, 1:2, 1:4, 1:6 and 1:8). The XRD studies confirmed that the synthesized samples had a mixture of Ni and NiO or single phase of NiO. The SEM observations confirmed that the composites were spherical in shape with an average size of about 70 nm for 1:1 mole ratio and about 40 nm for 1:8 mole ratio samples. At lower N:C mole ratios, the obtained samples had mixture of ferromagnetic Ni and NiO, while at high N:C mole ratios, the sample consisted of almost single phase of NiO. The formation of ferromagnetic Ni was attributed to reduction of some amount of NiO by residual carbon.

Keywords Sol–gel · Citric acid · Nanocomposite · Nickel · Nickel oxide

1 Introduction

Nanomaterials find extensive applications in energy conversion and storage, catalysis, sensing, imaging, magnetic

recording media, luminescence, etc., because of their unique physical and chemical properties [1–5]. The fascinating properties of nanomaterials arise due to increased surface area, surface to volume ratio (S/V) and changes in the electronic states. For example, as the grain size decreases, S/V ratio increases drastically. As a consequence, there is increase in dispersion (ratio of surface atoms to that of the bulk) and dangling state (missing bonds) [1–3]. Nanostructured transition-metal oxides such as NiO, CoO, CuO, ZnO, etc. are extensively studied for different applications during the past decade. Among them, NiO is a unique ceramic material which finds wide applications such as electrode material in Li-ion battery [3], electrochemical capacitors [6], catalysts [7], high-temperature gas sensors [8–11], etc. Nickel and nickel oxide (Ni/NiO) nanocomposite has also been utilized as catalyst in fuel cells [12]. It was reported that the use of Ni/NiO mixture as anode delivered better performance compared to pure NiO in Li-ion battery [3]. Cui and Lu [13] reported improved efficiency of hydrogen generation by using Ni/NiO mixture on TiO₂. Hu et al. [14] have used Ni/NiO mixture as internal reference for oxygen sensors. Rahulan et al. [15] utilized Ni/NiO mixture for nonlinear optical properties.

Both Ni and NiO crystallize in cubic phase. The magnetic state of metallic Ni is ferromagnetic, while NiO is antiferromagnetic in the bulk. The saturation magnetization (M_s) and coercivity field (H_c) of the bulk Ni are 55 emu g⁻¹ and 100 Oe, respectively [16, 17]. It is reported that these values are altered with decrease of grain size. For example, Niasari et al. [18, 19] reported M_s value of 54.2 emu g⁻¹ and H_c value of 19 Oe. The altered values were attributed to nanosize effect. The morphology (size, shape and distribution) has strong influence on chemical and physical properties of Ni and NiO. Several synthetic

K. Mahendraprabhu · P. Elumalai (✉)
Department of Green Energy Technology, Madanjeet School of
Green Energy Technologies, Pondicherry University, R.V.
Nagar, Puducherry 605014, India
e-mail: drperumalelumalai@gmail.com;
elumalai.get@pondiuni.edu.in

routes such as hydrothermal [6], thermal decomposition [19], microwave [20], sonochemical [21], sol–gel [22], etc. have been used to obtain different morphology. Among them, sol–gel is one of the wet-chemical facile methods with greater interest because of its simplicity, low cost and low temperature. The sol–gel chemistry involves solution-based route to obtain metal oxides with high porous and surface area at low temperature. Generally, metal precursor and gelling agent are mixed to form gel at low temperature. Calcination of the gel leads to formation of oxide matrix network with highly porosity. Wu et al. [23] reported the sol–gel synthesis of NiO. They have extensively studied various parameters such as pH, citric acid concentration, calcination time, temperature and heating rate. Thota and Kumar [24] studied the magnetic behavior of NiO nanoparticles obtained by sol–gel route using oxalic acid by varying the calcination temperatures. It was observed that the NiO nanoparticles exhibited superparamagnetic nature. Teoh and Li [25] prepared NiO nanoparticles using a block copolymer as surfactant via sol–gel route with varying calcination temperatures and H₂O concentrations. In all cases, mainly NiO was resulted even in different experimental conditions.

In the present investigation, sol–gel process was explored for generating Ni/NiO nanocomposite by varying nickel nitrate to citric acid mole ratio (N:C). Interestingly, it was observed that the N:C mole ratio had strong influence on the formation of Ni/NiO composition. The obtained samples were characterized by X-ray diffraction (XRD), scanning electron microscope (SEM), energy dispersive X-ray analysis (EDX), Fourier transformed infrared spectroscopy (FT-IR) and vibrating sample magnetometer (VSM) studies. For the first time, it was observed that the modulation of N:C mole ratio could produce either a mixture of ferromagnetic Ni and NiO almost in equal amount or single phase of NiO. The detailed sol–gel process and characterization studies are reported here.

2 Experimental

Citrate-based sol–gel method was used to prepare Ni/NiO nanocomposites. Chemicals such as nickel nitrate [Ni(NO₃)₂·6H₂O] and citric acid (C₆H₈O₇) were of analytical grade and used as received. Deionized water was used throughout the experiment. The nickel nitrate concentration was kept constant at 0.1 M, while the concentrations of citric acid were 0.1, 0.2, 0.4, 0.6 and 0.8 M, so as to obtain the mole ratios of nickel nitrate to citric acid (N:C) to be 1:1, 1:2, 1:4, 1:6 and 1:8. An appropriate quantity of nickel nitrate was dissolved in deionized water and stirred at 80 °C for an hour on hotplate for complete dissolution. To this hot solution, citric acid solution was

added in dropwise and then the temperature was increased to 130 °C to form the gel. Then, the gel was allowed to dry at the same temperature for overnight. Finally, the dried gel was subjected to calcination at 500 °C for 3 h in the air.

The crystal structure and phase purity of the obtained samples were characterized by powder XRD analysis by using diffractometer (Bruker D8 Advanced) equipped with Cu K_α radiation (wavelength, $\lambda = 1.5418 \text{ \AA}$). FT-IR spectroscopy data were obtained by using FT-IR spectroscopy (Thermo Nicolet 6700) in the frequency range of 400–4,000 cm⁻¹. The surface morphology and elemental analysis of the samples were carried out by using scanning-electron microscope equipped with elemental microanalysis system (SEM/EDX - Hitachi S3400N). The field dependent magnetization (M–H) curves were obtained by using VSM (Lake shore 7404).

3 Results and discussion

3.1 Crystal structure and morphology

The crystal structure and phase purity of the sol–gel derived powders were carried out by XRD. Figure 1 shows the XRD patterns of the samples obtained from each of the various N:C mole ratios. In all samples, XRD pattern consists of distinct Bragg peaks which indicate that the samples are crystalline in nature. For the samples obtained from lower N:C mole ratios (1:1 and 1:2), the set of Bragg peaks observed at diffraction angles (2 θ), 44.5°, 52.0° and 76.4° could be conveniently indexed to the cubic phase of Ni as per the standard JCPDS PDF # 897128, while the set of Bragg peaks appeared at 37.4°, 43.3°, 62.9°, 75.62° and 79.5° could be assigned to cubic phase of NiO as per the standard XRD pattern of JCPDS # 731519. On the contrary, for the samples obtained from the higher N:C mole ratios (1:4, 1:6 and 1:8), the set of peaks appeared at diffraction angles of 37.4°, 43.3°, 62.9°, 75.62° and 79.5° could be indexed to a single phase of NiO (JCPDS PDF # 731519). It is interesting to note that at lower N:C mole ratios (1:1 and 1:2), the sample consisted of a mixture of Ni and NiO, while at higher N:C mole ratios (1:4, 1:6 and 1:8), only single phase of cubic NiO was resulted. Thus, it is confirmed that citric acid concentration had strong influence on the formation of Ni/NiO composition in the sol–gel process. To the best of our knowledge, there are no reports on sol–gel process which observed a mixture of Ni and NiO. So far only nickel oxide was reported with insignificant amount of Ni at high citric acid concentration [23]. This is the first time the formation of Ni along with NiO almost in equal amount is observed in the sol–gel process. So, it is recommended for use of lower N:C mole ratio to obtain Ni/NiO composite and higher N:C mole

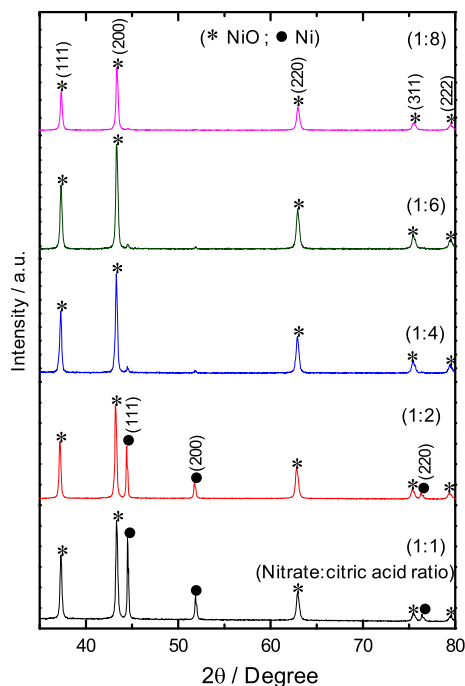


Fig. 1 XRD pattern of Ni/NiO composites synthesized by sol-gel process using each of various mole ratios of nitrate and citric acid

ratio for getting pure NiO. The crystallite sizes of each of NiO and Ni were calculated from their respective Bragg peaks by using Scherer formula given in Eq. (1).

$$L_{hkl} = 0.9 \lambda / \beta \cos \theta \quad (1)$$

where, L_{hkl} denotes crystallite size, λ is X-ray wavelength, β is the full width at half maximum (FWHM) of the Bragg peak (in radians), and θ is the Bragg angle. It was found that the average crystallite size was about 50 nm for Ni and 60 nm for NiO.

To identify the presence of undecomposed citrate molecules or partially decomposed products of citric acid and the metal-oxygen bond, FT-IR spectrum was recorded. Figure 2 shows the FT-IR spectra of the samples obtained from each of various N:C mole ratios. The strong peak appeared at 570 cm^{-1} confirms the presence of Ni-O bond in all the samples. The peak at $1,000 \text{ cm}^{-1}$ is characteristics for C-H bond which could have come from the precursor molecules or partially decomposed products of the precursor. It is noteworthy that as the N:C mole ratio increased, the intensity of the peak at $1,000 \text{ cm}^{-1}$ is increased significantly. This could be due to the presence of more amounts of partially decomposed products of citric acid. The peak at around $1,300 \text{ cm}^{-1}$ is due to presence of carbonyl band of metal-carboxylate stretch (carboxyl group of citric acid coordinated to Ni) [26].

The surface morphology of as-synthesized Ni/NiO samples was examined by SEM analysis. Figure 3 shows

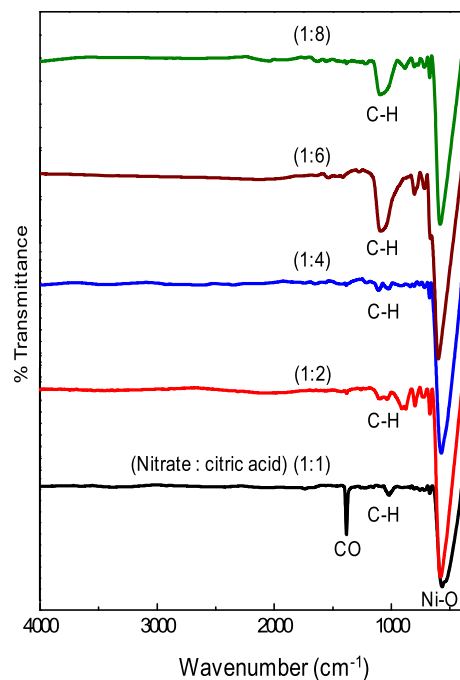


Fig. 2 FT-IR spectra of Ni/NiO composites synthesized by sol-gel process using each of various mole ratios of nitrate and citric acid

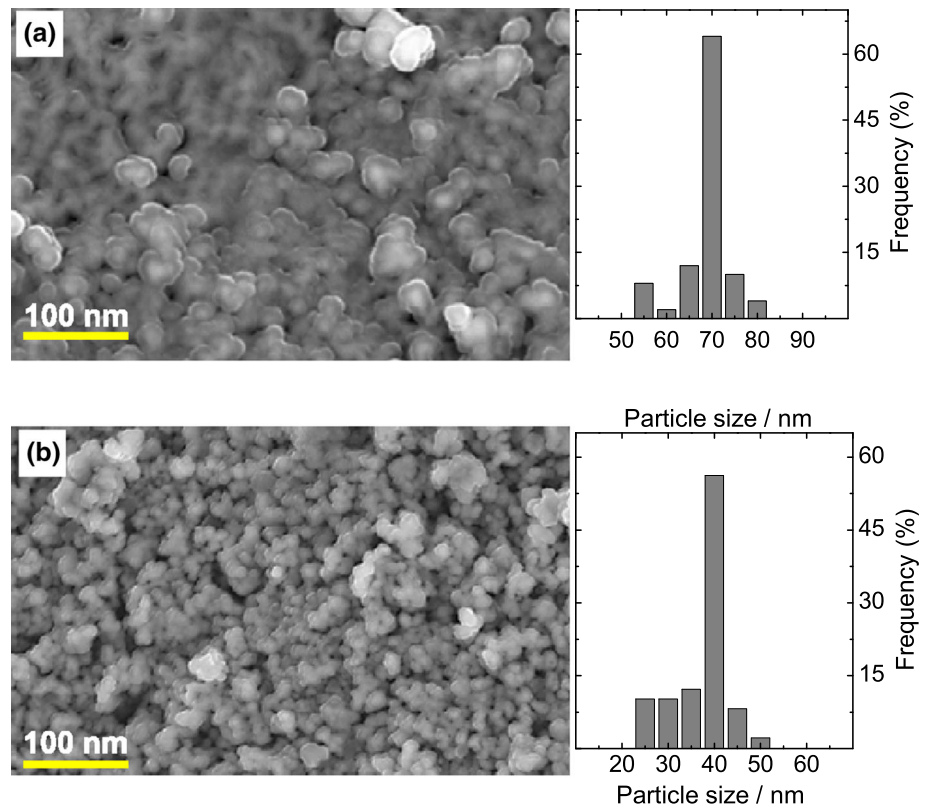
the representative SEM images of the samples obtained from N:C mole ratios, 1:1 and 1:8. It can be seen that the surface of the sample obtained from (1:1) N:C mole ratio consisted of almost uniform shape of spherical grains with average size of about 70 nm. Also, it is noted that the surface of the sample synthesized from higher N:C mole ratio (1:8), the grains are significantly lower in size (about 40 nm). To quantify the size distribution, size of particles from several SEM images was measured and plotted against frequency. The obtained histogram is given in Fig. 3. It can be seen that the size distribution is centered at about 70 and 40 nm for N:C mole ratios of (1:1) and (1:8), respectively.

The elemental composition examined by EDX analysis confirmed the presence of Ni as the only metallic element in the samples. Based on the aforementioned XRD, FT-IR and SEM/EDX results, it is confirmed that the N:C mole ratio had strong influence on the formation of Ni/NiO composition. Lower N:C mole ratios lead to a mixture of Ni and NiO, and higher N:C ratios lead to the single phase of NiO.

3.2 Magnetic properties of Ni/NiO nanocomposite

Since the use of low N:C mole ratio resulted in the formation of Ni/NiO mixture which has ferromagnetic Ni, the magnetic behavior of all the samples was studied by VSM technique. The obtained field dependent magnetization

Fig. 3 SEM images of Ni/NiO composites obtained by sol-gel process using **a** 1:1 and **b** 1:8 N:C mole ratios



(M–H) plots of all the samples are shown in Fig. 4a. It is seen that in the case of the samples obtained from the N:C mole ratios (1:1) and (1:2), as the field strength is increased, the magnetization increased and reaches a clear saturation. Upon the removal of magnetic field strength, the magnetization curve followed the path with significant hysteresis (shown in expanded view, Fig. 4b). The appearance of the hysteresis confirms the presence of ferromagnetic Ni in the sample. Interestingly, in the case of the samples obtained from higher N:C mole ratios, M–H plot did not have hysteresis. The absence of hysteresis loop is characteristics for superparamagnetic material in the sample. It is well known that when the grain size of magnetic material is reduced to nanoscale, it transforms into superparamagnetic [27]. Thus, it seems that, in the case of the samples synthesized from above 1:4 (N:C) mole ratios, the antiferromagnetic NiO is transformed into superparamagnetic due to nanosize effects. It is noteworthy that the hysteresis loop of (1:1) and (1:2) N:C mole ratio samples, is symmetric with respect to zero magnetic field (Fig. 4b). No significant displacement was observed. If there is ferromagnetic/antiferromagnetic coupling, there will be a displacement in the hysteresis loop towards left leading to shift in H_c value. The shift in H_c can be measured as exchange bias field (H_{eb}) [28]. It is noted that in the present work, there was no displacement in the

hysteresis loop which indicates that ferromagnetic/antiferromagnetic coupling is very weak at the measured temperature.

It is interesting to note the gradual change of saturation magnetization (M_s) with increase of N:C mole ratio (shown as inset in Fig. 4a). It is noted that as the N:C mole ratio increased, the M_s value decreased significantly. The sample consisting of Ni/NiO nanocomposites synthesized from (1:1) N:C mole ratio exhibited the highest saturation magnetization (28 emu g^{-1}). The highest M_s value is attributed to the presence of ferromagnetic Ni grains. In the case of the sample obtained from (1:2) N:C mole ratio, the M_s value is significantly less than that of the bulk, indicating size effect. The coercivity field of each sample is significantly different due to obvious size effect. It can be seen that the samples obtained from higher N:C mole ratios (above 1:4) exhibited very low M_s and H_c values due to superparamagnetic nature.

It is noted that the samples obtained from (1:1) and (1:2) N:C mole ratios annealed under air atmosphere, got attracted to the physical magnet. The magnetic attraction is due to presence of the ferromagnetic Ni. On contrary, the samples obtained from N:C mole ratios above (1:4) annealed under air atmosphere, hardly attracted. These observations substantiated the VSM results discussed above.

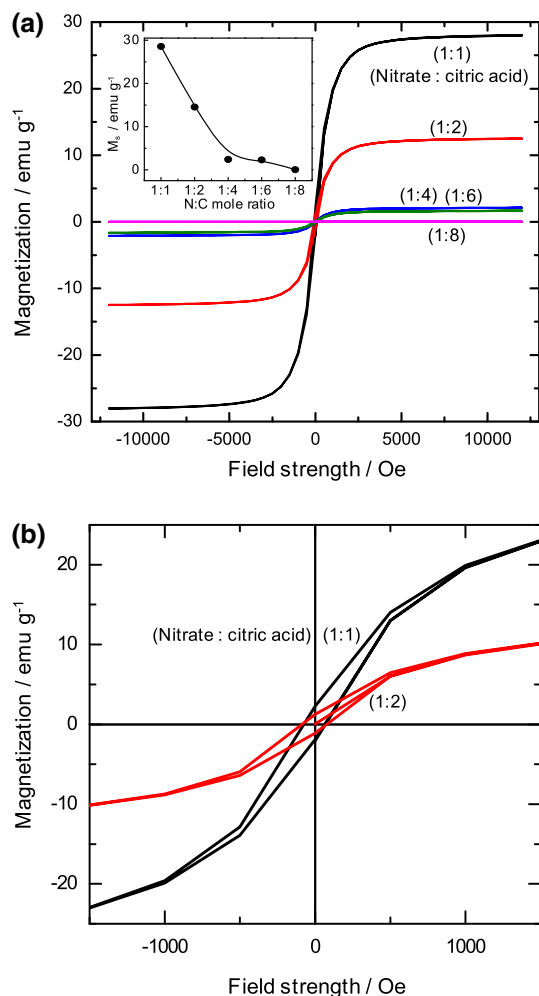


Fig. 4 **a** Field dependent magnetization curves recorded for the samples obtained from various N:C mole ratios and **b** expanded M–H curves for (1:1) and (1:2) N:C mole ratio samples. Inset dependence of M_s value on N:C mole ratio

3.3 Explanation for the formation of Ni/NiO composition

It was observed that the concentration of citric acid on nickel nitrate (N:C, mole ratio) had strong influence in the formation of Ni/NiO compositions. At lower N:C mole ratios (1:1 and 1:2), the sample consisted of a mixture of nanosize Ni and NiO. As the N:C mole ratio increased (1:4 and above), the sample consisted of almost single phase NiO. It is usually reported that the sol–gel process lead to the formation of metal oxides rather than metal. Interestingly, in the present investigation, at lower N:C mole ratio, a mixture of Ni/NiO was obtained. The formation of Ni could be due to reduction of some amount of NiO by the residual carbon (from citrate decomposition). It is expected that higher citric acid concentration would lead to formation of Ni metal, as more amount of residual carbon can

reduce NiO to Ni. So, it is believed that at higher N:C mole ratios, the high residual carbon content would have lead to complete reduction of NiO to Ni with reduced grain size (40 nm). Since nano metal grains are highly reactive, the formed Ni seemed to be completely oxidized to NiO. Thus, at higher N:C mole ratios (1:4 and above), single phase of NiO was resulted. It is expected that annealing under inert atmosphere would lead to formation of more Ni, irrespective of N:C mole ratios. So, to verify this as well as the above assumption, the dried gels were annealed under N_2 atmosphere. The obtained samples were characterized by XRD (not shown). It turned out that the (1:1) N:C mole ratio sample had more of Ni and the 1:8 mole ratio sample had almost equal amount of Ni and NiO. In the case of (1:8) N:C mole ratio sample, it was observed that the peaks of NiO (200) and Ni (111) were overlapping due to nanosize effect. It is noted that the (1:8) N:C mole ratio gel annealed under air resulted in NiO single phase (Fig. 1), while the gel annealed under N_2 had a mixture of Ni and NiO. In addition, it was found that the samples annealed under N_2 got attracted to physical magnet, irrespective of N:C mole ratios due to presence of ferromagnetic Ni. It seems that annealing under N_2 atmosphere lead to formation of more Ni, irrespective of N:C mole ratio by virtue of the inert atmosphere. This confirms oxidation of nano grain Ni under air annealing in the case of (1:8) N:C mole ratio.

4 Conclusion

It was demonstrated that N:C mole ratio had strong influence on the formation of Ni/NiO composition. In lower N:C mole ratios (1:1 and 1:2), a mixture of Ni and NiO and in higher N:C mole ratios, single phase of NiO was obtained. The samples synthesized from lower mole ratios (1:1 and 1:2) exhibited high M_s value because of the presence of ferromagnetic Ni, while the samples obtained from N:C mole ratios above (1:4), consisting of only NiO, exhibited superparamagnetic nature. The obtained Ni/NiO nanocomposites will be utilized for sensing of toxic gases at high temperature.

Acknowledgments Department of Science and Technology (DST), Govt. of India, New Delhi, is acknowledged for the financial support for the Fast-Track Grant (DST/FT/CS-64/2010). We extend our gratitude to CSIR-CECRI at Karaikudi and Chennai, and Central Instrumentation Facility - Pondicherry University for XRD and SEM measurements.

References

- Rao CNR, Govindaraj A, Vivekchand SRC (2006) Annu Rep Prog Chem Sect. A Inorg Chem 102:20–45

2. Bruce PG, Scrosati B, Tarascon JM (2008) *Angew Chem Int Ed* 47:2930–2946
3. Wen W, Wu JM, Cao MH (2013) *J Mater Chem A* 1:3881–3885
4. Fujio Y, CN Xu, Terasaki N, Ueno N (2014) *J Lumin* 148:89–93
5. Lim J, Murugan P, Lakshminarasimhan N, Kim JY, Lee JS, Lee SH, Choi W (2014) *J Catal* 310:91–99
6. Jiang Y, Chen D, Song J, Jiao Z, Maa Q, Zhang H, Cheng L, Zhao B, Chu Y (2013) *Electrochim Acta* 91:173–178
7. Yuan F, Ni Y, Zhang L, Yuan S, Wei J (2013) *J Mater Chem A* 1:8438–8444
8. Hua B, Chen W, Zhou J (2013) *Sens Actuators B Chem* 176:522–533
9. Mahendraprabhu K, Miura N, Elumalai P (2013) *Ionics* 19:1681–1686
10. Schelter M, Zosel J, Oelßner W, Gutha U, Mertig M (2013) *Sens Actuators B Chem* 187:209–214
11. Lee I, Choi SJ, Park KM, Lee SS, Choi S, Kim ID, Park CO (2014) *Sens Actuators B Chem* 197:300–307
12. Dutta A, Datta J (2014) *J Mater Chem A* 2:3237–3250
13. Cui E, Lu G (2014) *Int J Hydrogen Energy* 39:8959–8968
14. Hu Q, Jacobsen T, Hansen KV, Mogensen M (2012) *J Electrochem Soc* 159:B811–B817
15. Rahulan KM, Padmanathan N, Philip R, Balamurugan S, Kana-kam CC (2013) *Appl Surf Sci* 282:656–661
16. Deraz NM (2012) *Int J Electrochem Sci* 7:4608–4616
17. Hwang JH, Dravid VP, Teng MH, Host JJ, Elliott BR, Johnson DL, Mason TO (1997) *J Mater Res* 12:1076–1082
18. Niasari MS, Davar F, Fereshteh Z (2010) *J Alloys Compd* 494:410–414
19. Davar F, Fereshteh Z, Niasari MS (2009) *J Alloys Compd* 476:797–801
20. Ren Y, Gao L (2010) *J Am Ceram Soc* 93:3560–3564
21. Aslani A, Oroojpour V, Fallahi M (2011) *Appl Surf Sci* 257:4056–4061
22. Hu C, Gao Z, Yang X (2007) *J Sol-Gel Sci Technol* 44:171–176
23. Wu Y, He Y, Wu T, Chen T, Weng W, Wan H (2007) *Mater Lett* 61:3174–3178
24. Thota S, Kumar J (2007) *J Phys Chem Solids* 68:1951–1964
25. Teoh LG, Li KD (2012) *Mater Trans* 53:2135–2140
26. Ouyang JM, Deng SP (2003) *Dalton Trans* 2846–2851. doi:10.1039/B304319C
27. Proenca MP, Sousa CT, Pereira AM, Tavares PB, Ventura J, Vazquez M, Araujo JP (2011) *Phys Chem Chem Phys* 13:9561–9567
28. Dimitrov DV, Zhang S, Xiao JQ, Hadjipanayis GC, Prados C (1998) *Phys Rev B* 58:12090–12094